3. Li S, Huang L. Non-viral gene therapy; promises and challenges. *Gene Ther* 2000; **7**: 31–34.
4. Hwang SJ, Davis ME. Cationic polymers for gene delivery: designs for overcoming barriers to systemic administration. *Curr Opin Mol Ther* 2001; **3**: 183–191.
5. Pannier AK, Shea LD. Controlled release systems for DNA delivery. *Mol Ther* 2004; **10**: 19–26.
6. Han S, Mahato RI, Sung YK, Kim SW. Development of biomaterials for gene therapy. *Mol Ther* 2000; **2**: 302–317.
7. Qiang B, Segev A, Beliard I, Nili N, Strauss BH, Sefton MV. Poly(methylidene malonate 2.1.2) nanoparticles: a biocompatible polymer that enhances peri-adventitial adenoviral gene delivery. *J Control Release* 2004; **98**: 447–455.
8. Han S, Mahato RI, Kim SW. Water-soluble lipopolymer for gene delivery. *Bioconjugate Chem* 2001; **12**: 337–345.
9. Lim YB, Kim SM, Suh H, Park JS. Biodegradable, endosome disruptive, and cationic network-type polymer as a highly efficient and nontoxic gene delivery carrier. *Bioconjugate Chem* 2002; **13**: 952–957.
10. Le Doux JM, Landazuri N, Yarmush ML, Morgan JR. Complexation of retrovirus with cationic and anionic polymers increases the efficiency of gene transfer. *Hum Gene Ther* 2001; **12**: 1611–1621.
11. Koping-Hoggard M, Tubulekas I, Guan H, *et al.* Chitosan as a nonviral gene delivery system. Structure-property relationships and characteristics compared with polyethylenimine in vitro and after lung administration in vivo. *Gene Ther* 2001; **8**: 1108–1121.
12. Wang J, Zhang PC, Mao HQ, Leong KW. Enhanced gene expression in mouse muscle by sustained release of plasmid DNA using PPE-EA as a carrier. *Gene Ther* 2002; **9**: 1254–1261.
13. Sano A, Maeda M, Nagahara S, *et al.* Atelocollagen for protein and gene delivery. *Adv Drug Deliv Rev* 2003; **55**: 1651–1677.
14. Honma K, Ochiya T, Nagahara S, *et al.* Atelocollagen-based gene transfer in cells allows high-throughput screening of gene functions. *Biochem Biophys Res Commun* 2001; **289**: 1075–1081.
15. Nguyen JB, Sanchez-Pernaute R, Cunningham J, Bankiewicz KS. Convection-enhanced delivery of AAV-2 combined with heparin increases TK gene transfer in the rat brain. *Neuroreport* 2001; **12**: 1961–1964.
16. Kichler A. Gene transfer with modified polyethylenimines. *J Gene Med* 2004; **6**: S3–10.
17. Fischer D, Bieber T, Li Y, Elsasser HP, Kissel T. A novel nonviral vector for DNA delivery based on low molecular weight, branched polyethylenimine: effect of molecular weight on transfection efficiency and cytotoxicity. *Pharm Res* 1999; **16**: 1273–1279.
18. Sweeney P, Karashima T, Ishikura H, *et al.* Efficient therapeutic gene delivery after systemic administration of a novel polyethylenimine/DNA vector in an orthotopic bladder cancer model. *Cancer Res* 2003; **63**: 4017–4020.
19. Ogris M, Brunner S, Schuller S, Kircheis R, Wagner E. PEGylated DNA/transferrin-PEI complexes: reduced interaction with blood components, extended circulation in blood and potential for systemic gene delivery. *Gene Ther* 1999; **6**: 595–605.
20. Hosseinkhani H, Aoyama T, Ogawa O, Tabata Y. Ultrasound enhancement of in vitro transfection of plasmid DNA by a cationized gelatin. *J Drug Target* 2002; **10**: 193–204.
21. Hosseinkhani H, Tabata Y. In vitro gene expression by cationized derivatives of an artificial protein with repeated RGD sequences, pronectin. *J Control Release* 2003; **86**: 169–182.
22. Fukunaka Y, Iwanaga K, Morimoto K, Kakemi M, Tabata Y. Controlled release of plasmid DNA from cationized gelatin hydrogels based on hydrogel degradation. *J Control Release* 2002; **80**: 333–343.
23. Wagner E. Strategies to improve DNA polyplexes for in vivo gene transfer: will "artificial viruses" be the answer? *Pharm Res* 2004; **21**: 8–14.
24. Mahato RI, Anwer K, Tagliaferri F, *et al.* Biodistribution and gene expression of lipid/plasmid complexes after systemic administration. *Hum Gene Ther* 1998; **9**: 2083–2099.
25. Pun SH, Davis ME. Development of a nonviral gene delivery vehicle for systemic application. *Bioconjugate Chem* 2002; **13**: 630–639.
26. Takakura Y, Nishikawa M, Yamashita F, Hashida M. Development of gene drug delivery systems based on pharmacokinetic studies. *Eur J Pharm Sci* 2001; **13**: 71–76.
27. Bragonzi A, Boletta A, Biffi A, *et al.* Comparison between cationic polymers and lipids in mediating systemic gene delivery to the lungs. *Gene Ther* 1999; **6**: 1995–2004.
28. Liu F, Qi H, Huang L, Liu D. Factors controlling the efficiency of cationic lipid-mediated transfection in vivo via intravenous administration. *Gene Ther* 1997; **4**: 517–523.
29. Nishikawa M, Huang L. Nonviral vectors in the new millennium: delivery barriers in gene transfer. *Hum Gene Ther* 2001; **12**: 861–870.
30. Tabata Y, Nagano A, Ikada Y. Biodegradation of hydrogel carrier incorporating fibroblast growth factor. *Tissue Eng* 1995; **5**: 127–138.
31. Okada Y. Sendai-virus induced cell fusion. *Methods Enzymol* 1993; **221**: 18–41.
32. Kaneda Y, Nakajima T, Nishikawa T, *et al.* Hemagglutinating virus of Japan (HVJ) envelope vector as a versatile gene delivery system. *Mol Ther* 2002; **6**: 219–226.
33. Saeki Y, Wataya-Kaneda M, Tanaka K, Kaneda Y. Sustained transgene expression in vitro and in vivo using an Epstein-Barr virus replicon vector system combined with HVJ liposomes. *Gene Ther* 1998; **5**: 1031–1037.
34. Shpetner H, Joly M, Hartley D, Corvera S. Potential sites of PI-3 kinase function in the endocytic pathway revealed by the PI-3 kinase inhibitor, wortmannin. *J Cell Biol* 1996; **132**: 595–605.
35. Chen X, Wang Z. Regulation of intracellular trafficking of the EGF receptor by Rab5 in the absence of phosphatidylinositol 3-kinase activity. *EMBO Rep* 2001; **2**: 68–74.
36. Saeki Y, Matsumoto N, Nakano Y, Mori M, Awai K, Kaneda Y. Development and characterization of cationic liposomes conjugated with HVJ (Sendai virus): reciprocal effect of cationic lipid for in vitro and in vivo gene transfer. *Hum Gene Ther* 1997; **8**: 2133–2141.
37. Yang YW, Hsieh YC. Protamine sulfate enhances the transduction efficiency of recombinant adeno-associated virus-mediated gene delivery. *Pharm Res* 2001; **18**: 922–927.
38. Merdan T, Kopecek J, Kissel T. Prospects for cationic polymers in gene and oligonucleotide therapy against cancer. *Adv Drug Deliv Rev* 2002; **54**: 715–758.
39. Maruyama K, Iwasaki F, Takizawa T, *et al.* Novel receptor-mediated gene delivery system comprising plasmid/protamine/sugar-containing polyanion ternary complex. *Biomaterials* 2004; **25**: 3267–3273.
40. Putnam D, Gentry CA, Pack DW, Langer R. Polymer-based gene delivery with low cytotoxicity by a unique balance of side-chain termini. *Proc Natl Acad Sci U S A* 2001; **98**: 1200–1205.
41. Hofland HE, Masson C, Iginla S, *et al.* Folate-targeted gene transfer in vivo. *Mol Ther* 2002; **5**: 739–744.
42. Su J, Kim CJ, Ciftci K. Characterization of poly((N-trimethylammonium)ethyl methacrylate)-based gene delivery systems. *Gene Ther* 2002; **9**: 1031–1036.
43. Schakowski F, Gorschluter M, Junghans C, *et al.* A novel minimal-size vector (MIDGE) improves transgene expression in colon carcinoma cells and avoids transfection of undesired DNA. *Mol Ther* 2001; **3**: 793–800.
44. Wang J, Zhang PC, Lu HF, *et al.* New polyphosphoramidate with a spermidine side chain as a gene carrier. *J Control Release* 2002; **83**: 157–168.
45. Yun YH, Goetz DJ, Yellen P, Chen W. Hyaluronan microspheres for sustained gene delivery and site-specific targeting. *Biomaterials* 2004; **25**: 147–157.
46. Kaneo Y, Tanaka T, Nakano T, Yamaguchi Y. Evidence for receptor-mediated hepatic uptake of pullulan in rats. *J Control Release* 2001; **70**: 365–373.
47. Hosseinkhani H, Aoyama T, Ogawa O, Tabata Y. Liver targeting of plasmid DNA by pullulan conjugation based on metal coordination. *J Control Release* 2002; **83**: 287–302.
48. Mikkelsen JG, Yant SR, Meuse L, Huang Z, Xu H, Kay MA. Helper-independent *Sleeping Beauty* transposon-transposase vectors for efficient nonviral gene delivery and persistent gene expression *in vivo*. *Mol Ther* 2003; **8**: 654–665.
49. Zhang G, Budker V, Wolff JA. High levels of foreign gene expression in hepatocytes after tail vein injections of naked plasmid DNA. *Hum Gene Ther* 1999; **10**: 1735–1737.
50. Fujita F, Yamashita-Futsuki I, Eguchi S, *et al.* Inactivation of porcine endogenous retrovirus by human serum as a function of complement activated through the classical pathway. *Hepatol Res* 2003; **26**: 106–113.

51. Okada H, Wu X, Okada N. Complement-mediated cytolysis and azidothymidine are synergistic in HIV-1 suppression. *Int Immunol* 1998; **10**: 91–95.
52. Ishida T, Yasukawa K, Kojima H, Harashima H, Kiwada H. Effect of cholesterol content in activation of the classical versus the alternative pathway of rat complement system induced by hydrogenated egg phosphatidylcholine-based liposomes. *Int J Pharm* 2001; **224**: 69–79.

Gene Therapy (2005), 1–9

www.nature.com/gt

ORIGINAL ARTICLE

Liver-directed gene therapy of diabetic rats using an HVJ-E vector containing EBV plasmids expressing insulin and GLUT 2 transporter

YD Kim[1,7], K-G Park[1,7], R Morishita[2], Y Kaneda[2], S-Y Kim[3], D-K Song[3], H-S Kim[1], C-W Nam[1], HC Lee[4], K-U Lee[5], J-Y Park[5], B-W Kim[6], J-G Kim[6] and I-K Lee[6]

[1]*Department of Internal Medicine & Institute for Medical Sciences, Keimyung University School of Medicine, Daegu, South Korea;* [2]*Division of Gene Therapy Science, Osaka University Medical School, Osaka, Japan;* [3]*Department of Physiology, Keimyung University School of Medicine, Daegu, South Korea;* [4]*Department of Internal Medicine, Yonsei University College of Medicine, Seoul, South Korea;* [5]*Department of Internal Medicine, University of Ulsan College of Medicine, Seoul, South Korea and* [6]*Department of Internal Medicine, Kyungpook National University School of Medicine, Daegu, South Korea*

Insulin gene therapy in clinical medicine is currently hampered by the inability to regulate insulin secretion in a physiological manner, the inefficiency with which the gene is delivered, and the short duration of gene expression. To address these issues, we injected the liver of streptozotocin-induced diabetic rats with hemagglutinating virus of Japan-envelope (HVJ-E) vectors containing Epstein–Barr virus (EBV) plasmids encoding the genes for insulin and the GLUT 2 transporter. Efficient delivery of the genes was achieved with the HVJ-E vector, and the use of the EBV replicon vector led to prolonged hepatic gene expression. Blood glucose levels were normalized for at least 3 weeks as a result of the gene therapy. Cotransfection of GLUT 2 with insulin permitted the diabetic rats to regulate their blood glucose levels upon exogenous glucose loading in a physiologically appropriate manner and improved postprandial glucose levels. Moreover, cotransfection with insulin and GLUT 2 genes led to in vitro *glucose-stimulated insulin secretion that involved the closure of* K_{ATP} *channels. The present study represents a new way to efficiently deliver insulin gene* in vivo *that is regulated by ambient glucose level with prolonged gene expression. This may provide a basis to overcome limitations of insulin gene therapy in humans.*

Gene Therapy advance online publication, 22 September 2005; doi:10.1038/sj.gt.3302644

Keywords: *insulin; GLUT 2; HVJ-E; EBV; diabetes*

Introduction

Insulin replacement is essential for maintaining the health of patients with type I diabetes mellitus. Many patients with type II diabetes also require insulin to control their blood glucose levels. Recent progress in molecular biology has fostered the development of gene therapy as a new therapeutic strategy.[1–3] Diabetes mellitus has long been considered to be curable with insulin gene therapy.[4,5] However, several unsolved problems currently hamper the use of insulin gene therapy in clinical practice. First, to regulate blood glucose levels without risking the development of hypoglycemia, any insulin secretion derived from the vector construct must be regulated by changes in blood glucose levels. Second, the gene expression vector used must be capable of prolonged expression. Third, an efficient and minimally invasive vector delivery system is required.

With regard to the first of these issues, recent studies have reported that insulin secretion from genes delivered to the liver can be controlled at the transcriptional level by blood glucose levels.[6–8] However, the drawback of this system is that the slow transcriptional regulation of this hepatic insulin gene expression delays the responsiveness of the plasma insulin levels to blood glucose changes.[6] Notably, Liu *et al.*[9] recently demonstrated that cotransfection a hepatoma cell line with the insulin and GLUT 2 transporter genes induces ATP-sensitive potassium (K_{ATP}) channels and leads to glucose-stimulated insulin secretion. Thus, cotransfection with the GLUT 2 gene may result in more timely glucose-regulated secretion of the insulin encoded by the insulin transgene.

With regard to the second of the issues hampering gene therapy, prolonged gene expression has been achieved by employing an Epstein–Barr virus (EBV)-based plasmid. The application of this plasmid in various cells has been developed.[10–12] EBV is of particular interest as a vector because of its latent infection property, which is characterized by autonomous replication and nuclear retention of the EBV genome in host cells.[13] The persistent maintenance of the EBV genome has been

Correspondence: Professor I-K Lee, Department of Internal Medicine, Kyungpook National University School of Medicine, 50, Samduk-2ga, Jung-gu, Daegu 700-721, South Korea.
E-mail: leei@knu.ac.kr
[7]These authors contributed equally to this work.
Received 16 March 2005; revised 14 July 2005; accepted 10 August 2005

analyzed in depth and is mediated by the replication origin of the latent viral DNA (oriP) and EBV nuclear antigen 1 (EBNA-1).[14,15] Previously, our group showed that use of the EBV replicon vector leads to sustained transgene expression *in vivo* in the liver.[11]

With regard to efficient vector delivery, numerous viral and nonviral vectors have been developed.[4] Adenovirus-mediated gene transfer has been successful in transiently expressing transgenes, but it also causes undesired effects such as hepatic inflammation.[16,17] Adeno-associated virus (AAV) is an attractive choice for insulin gene therapy. A recent study showed the safety and efficacy of AAV-mediated insulin gene transfer into streptozotocin (STZ)-induced diabetic rats.[18] Although AAVs generally have low immunogenicity,[19] a potential caveat of this approach is the possible generation of neutralizing antibody that might limit readministration. In addition, a large proportion of the human population has pre-existing antibodies against AAV that may limit gene transfer by this virus.[4,20] Nonviral vectors are less toxic and less immunogenic,[21] but most are also less efficient, especially *in vivo*. Gene therapy strategies employing the hemagglutinating virus of Japan (HVJ)-liposome system have recently met with success in animals.[22–25] Also, Kaneda *et al.* recently developed the HVJ-envelope (HVJ-E) vector system, which is a simple method to convert an inactivated virus containing lipid envelop into gene transfer vector. They used this technology to introduce plasmid DNA directly into inactivated HVJ-E and investigated the feasibility of using this HVJ-E vector for gene transfer. HVJ-E vector is even more effective than HVJ-liposomes for *in vivo* gene transfer.[26] Finally, gene transfer to the liver, lung, uterus, eye, skin, muscle and brain of animals such as rat, mouse, rabbit and monkey has been achieved by the direct injection of the HVJ-E vector. Among the various organs tested, HVJ-E vector was more effective than HVJ-liposome for gene transfer to the liver, uterus, brain and lung.

Here, we show the efficacy of cotransfecting hepatic cells with an EBV replicon vector encoding human insulin and GLUT 2 transporter (referred to here as pEBAct-ins and pEBAct-glut2, respectively) by using the HVJ-E vector. Significantly, this novel gene therapy was highly effective in treating hyperglycemia in STZ-induced diabetic rats. Moreover, cotransfected diabetic rats were able to regulate their glucose levels in response to exogenous glucose levels in a physiologically appropriate manner.

Results

Hepatic insulin and GLUT 2 gene expression

We examined the effectiveness of *in vivo* gene transfer by immunohistochemical analysis of insulin and GLUT 2 proteins. We directly injected the HVJ-E vector bearing pEBAct-ins with or without pEBAct-glut2 into the STZ-induced diabetic rat liver. At 4 days after the transfection of pEBAct-ins with or without pEBAct-glut2, the rat liver showed expression of insulin (Figure 1b and c). In contrast, in the control vector-transfected rat, positive

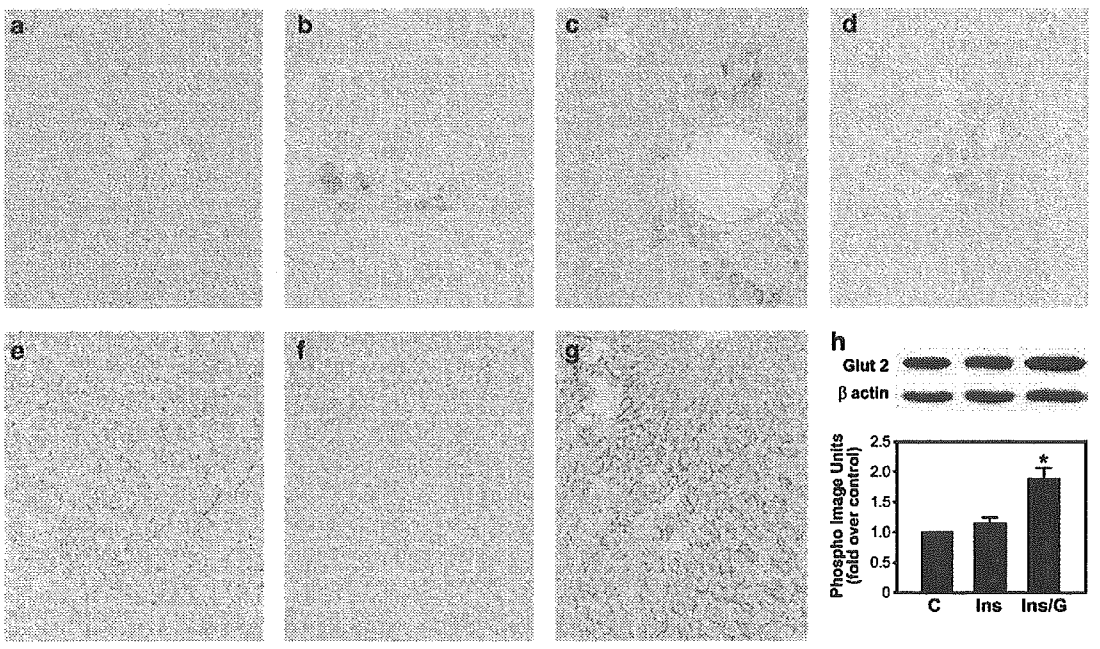

Figure 1 Hepatic insulin and GLUT 2 gene expression. (**a–g**) Immunohistochemistry. Anti-insulin antibody (**a–d**) or anti-GLUT2 antibody (**e–g**) staining of liver sections from STZ-induced diabetic rats treated with control vector (**a, e**), pEBAct-ins (**b, f**), or pEBAct-ins plus pEBAct-glut2 (**c, g**) and killed 4 days later. (**d**) Anti-insulin antibody staining of liver sections from a STZ-induced diabetic rat treated with pEBAct-ins plus pEBAct-glut2 and killed 25 days later. (**h**) Western blot analysis of hepatic GLUT 2 expression in diabetic control transfected with control vector and in STZ-induced diabetic rats treated with pEBAct-ins with or without pEBAct-glut2. Total protein was extracted from the indicated tissues 4 days after treatment and subjected to Western blot analysis as described in the Materials and methods. The data were quantified and expressed as means ± s.e.m. of five separate measurements (lower panels). C, STZ-induced diabetic rats treated with control vector; Ins, STZ-induced diabetic rats treated with pEBAct-ins; Ins/G, STZ-induced diabetic rats treated with pEBAct-ins plus pEBAct-glut2. Statistically significant differences compared with C are indicated by $^*P<0.01$.

staining was not observed (Figure 1a). Moreover, prolonged *in vivo* insulin gene expression was achieved by using the EBV replicon vector, as shown by the rat liver harvested 25 days after transfection (Figure 1d). The liver cells normally expressed GLUT 2 (Figure 1e). Transfection with pEBAct-ins did not affect GLUT 2 expression levels, but transfection with pEBAct-glut2 markedly increased expression (Figure 1g). These results were confirmed by Western blot analysis of GLUT 2 protein levels in primary isolated hepatocytes at 4 day after transfection (Figure 1h).

Effect of cotransfecting insulin and GLUT 2 on blood glucose levels and body weight in STZ-induced diabetic rats

STZ-induced diabetic rats showed extremely high fasting blood glucose levels that rose to 20.82 ± 0.39 mmol/l. In the rats treated with pEBAct-ins (with or without pEBAct-glut2), the fasting blood glucose levels dropped dramatically, close to the levels observed in nondiabetic rats (Figure 2a). Normal blood glucose levels were maintained until 22 days after treament, until which point the glucose levels did not significantly differ from those of nondiabetic rats (Figure 2a). The addition of pEBAct-glut2 to pEBAct-ins did not alter the fasting glucose levels.

While STZ treatment markedly reduced body weight, insulin-vector treatment induced a progressive gain in body weight. Notably, the addition of pEBAct-glut2 to the insulin treatment enhanced the rate of weight gain to the point statistically significant differences between the pEBAct-ins alone (Ins) and pEBAct-ins/-glut2 rats (Ins/G) started to be observed from day 20 to day 25 (Figure 2b).

Plasma insulin and C-peptide levels

To confirm that the hypoglycemic effects observed are due to hepatic insulin gene expression, we measured plasma insulin and C-peptide levels in 8 h-fasting rats treated or not with the insulin gene. At 4 days after treatment, negligible amounts of rat insulin and C-peptide were found in the plasma of the STZ-induced diabetic rats, irrespective of whether or not they were treated with the insulin gene. In contrast, significant amounts of human insulin and C-peptide were detected in the plasma of diabetic Ins and Ins/G rats, indicating *de novo* synthesis from the delivered gene (Figure 3). At day 25, plasma insulin levels decreased to ~40% of the day 4 levels (Figure 3a), which was also reflected by the increased blood glucose levels (Figure 2a).

Glucose responsiveness of the hypoglycemia induced by pEBAct-ins/-glut2 cotransfection

We examined whether cotransfecting pEBAct-ins and pEBAct-glut2 helps the diabetic rat to regulate its blood glucose levels in response to exogenous glucose loading. The intraperitoneal glucose tolerance test (IPGTT) revealed that the blood glucose levels of diabetic Ins/G rats peaked within 60 min and then decreased at 120 min, similar to the glucose levels of nondiabetic control rats. In diabetic Ins rats, fasting blood glucose levels were similar to those of control and diabetic Ins/G rats. However, the blood glucose levels at 120 min were significantly higher than those of nondiabetic control

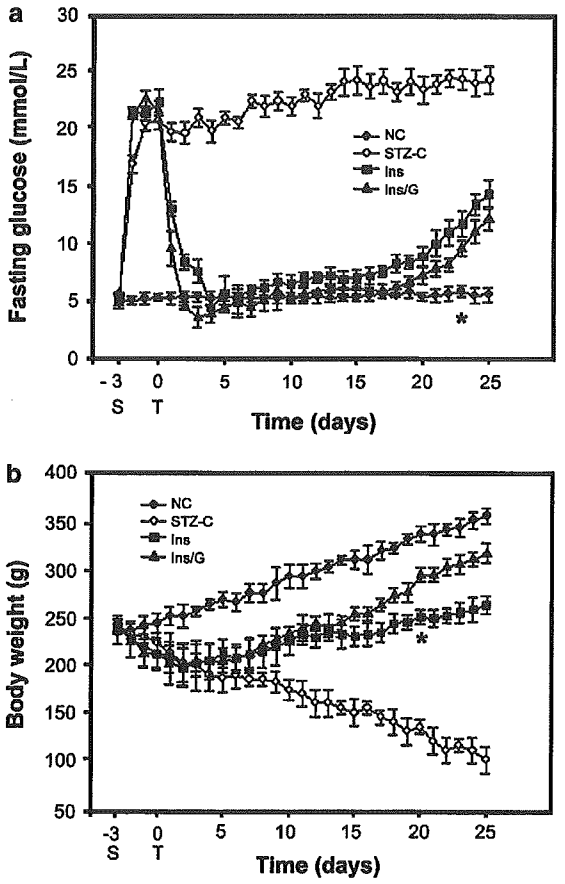

Figure 2 Effect of insulin and GLUT 2 vector transfection on fasting blood glucose levels and body weight. At 8-h-fasting blood glucose levels (**a**) and body weights (**b**) in STZ-induced diabetic rats ($n = 5$ per group) were measured daily after injecting the indicated vector(s). NC, nondiabetic control rats; STZ-C, STZ-induced diabetic rats treated with control vector; Ins, STZ-induced diabetic rats treated with pEBAct-ins; Ins/G, STZ-induced diabetic rats treated with pEBAct-ins plus pEBACt-glut2; S, STZ injection day; T, day of treatment with pEBAct-ins with or without pEBAct-glut2. Values shown are means $\pm$ s.e.m. Statistically significant differences compared with Ins/G are indicated by $^*P < 0.05$.

or diabetic Ins/G rats (Figure 4a). We also measured 2 h-postprandial glucose levels on day 4 and day 22. The rats were fasted for 12 h and then given dietary chow from 6 pm. Glucose levels measured at 8 pm showed that postprandial glucose levels in diabetic Ins/G rats were significantly lower than those in diabetic Ins rats (Figure 4b).

Stimulation of insulin secretion by glucose and glibenclamide

We asked whether the glucose-responsive hypoglycemia induced by pEBAct-ins/-glut2 cotransfection is mediated by glucose-stimulated insulin secretion. For this purpose, we transfected HepG2 human hepatoma cells with pEBAct-ins alone (HepG2ins) or with pEBAct-glut2 (HepG2ins/g). As shown in Figure 5a, the basal (5 mM glucose) insulin secretion of HepG2ins/g cells did not differ from that of HepG2ins cells. The static stimulation

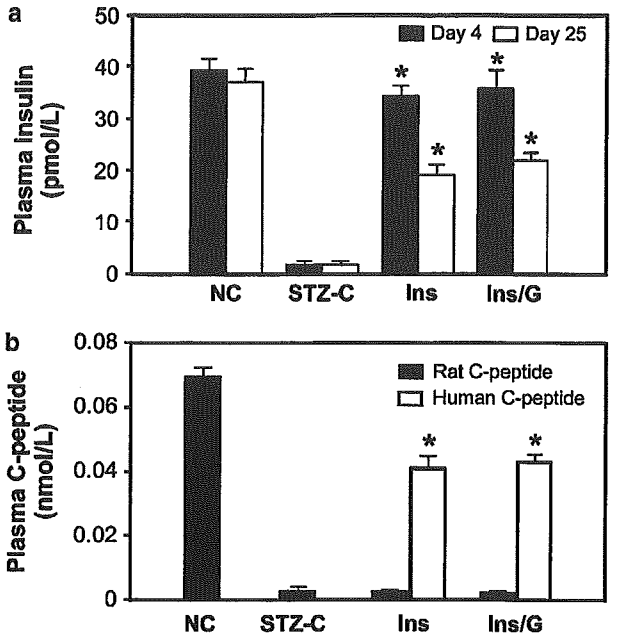

Figure 3 Effect of insulin and GLUT 2 vector transfection on plasma insulin and C-peptide levels. Four or 25 days after treatment, 8 h fasting plasma insulin (**a**) and C-peptide (**b**) levels ($n=5$ per group) were measured as described in the Materials and methods. NC, nondiabetic control rats; STZ-C, STZ-induced diabetic rats treated with control vector; Ins, STZ-induced diabetic rats treated with pEBAct-ins; Ins/G, STZ-induced diabetic rats treated with pEBAct-ins plus pEBACt-glut2. Values are shown means ± s.e.m. Statistically significant differences compared to STZ-C are indicated by $^*P<0.001$.

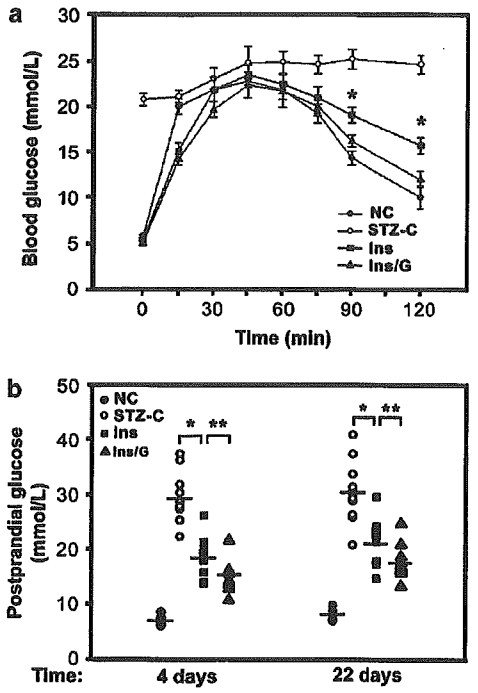

Figure 4 Glucose responsiveness of the hypoglycemia induced by cotransfecting the insulin and GLUT 2 vectors. (**a**) Intraperitoneal glucose tolerance test. The indicated rats were loaded intraperitoneally with glucose (2 g/kg) after a 6 h fast and blood glucose levels were measured at the indicated time points. Statistically significant differences compared with Ins are indicated by $^*P<0.01$. (**b**) Postprandial glucose levels. Rats were fasted for 12 h before feeding and then 2-h-postprandial glucose levels were measured on day 4 and 22 after gene therapy. Horizontal bars mark the mean for each group ($n=10$). $^*P<0.001$ and $^{**}P<0.01$. NC, nondiabetic control rats; STZ-C, STZ-induced diabetic rats treated with control vector; Ins, STZ-induced diabetic rats treated with pEBAct-ins; Ins/G, STZ-induced diabetic rat treated with pEBAct-ins plus pEBACt-glut2.

of HepG2ins/g with 25 mM glucose for 1 h significantly increased insulin secretion relative to the basal glucose level. In contrast, the static stimulation with 25 mM glucose did not increase the insulin secretion by HepG2ins cells. Thus, these data suggest that cotransfection of hepatic cells with pEBAct-ins/-glut2 elevates their glucose-responsive insulin secretion. We next examined the changes in plasma insulin levels in response to glibenclamdie. As shown in Figure 5b, plasma insulin levels of nondiabetic control rats gradually increased and peaked at 90 min after intraperitoneal glibenclamide administration. A similar trend was observed in diabetic Ins/G rats, even though the level of stimulation by glibenclamide was lower than in diabetic Ins/G rats. On the other hand, plasma insulin levels in diabetic Ins rats were not affected by glibenclamide. These data suggest that insulin secretion from hepatocytes in Ins/G rats was mediated by functional K_{ATP} channels (see below).

Response of whole-cell membrane currents to high glucose stimulation

We next, investigated whether the *in vivo* and *in vitro* glucose-responsive insulin secretion induced by insulin and GLUT 2 vector cotransfection is mediated by functional K_{ATP} channels. For this purpose, we measured the K_{ATP} channel current in empty-vector-transfected HepG2, HepG2ins and HepG2ins/g cells by using the whole-cell patch-clamp technique (Figure 6). The 200-ms ramp pulses from −100 to +80 mV were applied at a holding potential of −50 mV. To amplify the current through the K_{ATP} channel, the channel-specific opener diazoxide (300 μM) was added to the bath solution prior to glucose application. The reversal potentials of the currents in the presence of diazoxide were around −40 ~ to −50 mV in the three different cells, which suggests they are mainly K^+ currents. In addition, the recorded current was much greater in HepG2ins/g cells compared to that in the empty-vector-transfected HepG2 control and HepG2ins cells, implying that functional K_{ATP} channel is more presented in the cell membrane of HepG2ins/g cells. When 20 mM glucose was added, the diazoxide-induced current was inhibited (Figure 6b), suggesting that the K_{ATP} channel responds to increase in ATP level by glucose in HepG2ins/g cells.

Liver toxicity analysis of HVJ-E vector containing EBV plasmid

As shown in Table 1, elevations in liver function parameters were found in STZ-induced diabetic rats on day 4 and day 22, respectively. This was in contrast to STZ-induced diabetic rats, diabetic Ins and Ins/G rats,

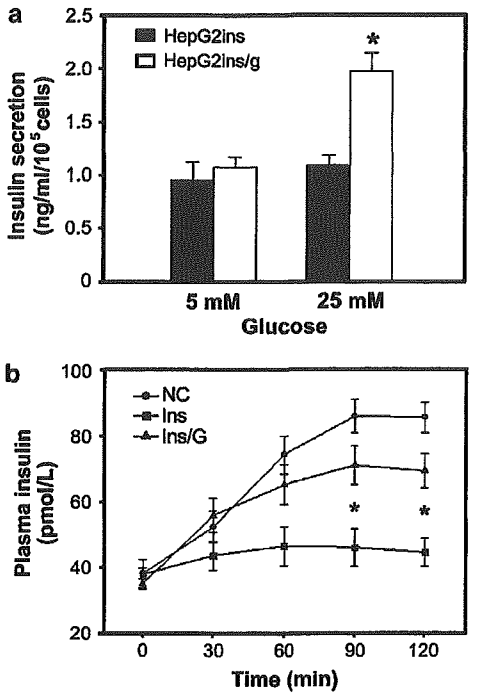

Figure 5 Stimulation of insulin secretion by glucose and glibenclamide (a) Effect of static stimulation with glucose on insulin secretion by HepG2 cells. HepG2 cells were transfected with pEBAct-ins with (HepG2ins/g) or without pEBAct-glut 2 (HepG2ins) and then treated with 5 or 25 mM glucose. Insulin secretion was determined as described in the Materials and methods. Statistically significant differences compared with HepG2ins are indicated by $^*P<0.01$. The values shown are means±s.e.m. ($n=4$). (b) Effect of glibenclamide on plasma insulin levels. The indicated rats were intraperitoneally administered glibenclamide (10 mg/kg) after a 6 h fast and plasma insulin levels were measured at the indicated time points. NC, nondiabetic control rats; STZ-C, STZ-induced diabetic rats treated with control vector; Ins, STZ-induced diabetic rats treated with pEBAct-ins; Ins/G, STZ-induced diabetic rat treated with pEBAct-ins plus pEBACt-glut2. Statistically significant differences compared with Ins are indicated by $^*P<0.05$. The values shown are means±s.e.m. ($n=5$ for each group).

which showed no relative changes in these parameters at day 4. Moreover, insulin gene transfer significantly improved these parameters on day 22 compared to STZ-induced diabetic rats. A histological examination on day 22 of the liver tissue of diabetic Ins/G rats revealed no detectable damage, whereas liver tissue from STZ-induced diabetic rat showed mild infiltration by inflammatory cells (data not shown).

Discussion

In the present study, we developed an alternative insulin gene transfection strategy that may be potentially more feasible in a clinical setting than existing strategies. This strategy involved direct liver injection of an HVJ-E vector bearing EBV replicon vectors encoding the insulin and GLUT 2 genes. Here, we report that application of this strategy to STZ-induced diabetic rats resulted in prolonged hepatic insulin gene expression and sustainted lowering of blood glucose levels. Moreover, we showed that when GLUT 2 was cotransfected with insulin, the blood glucose levels rose upon exogenous glucose loading and then returned to baseline with kinetics that resembled those in nondiabetic rats. In addition, postprandial glucose control in diabetic rats cotransfected with insulin and GLUT 2 was better than in diabetic rats transfected with insulin alone. We also showed that these effects are likely to be mediated by glucose-stimulated insulin secretion.

Pancreatic beta cells represent a highly differentiated cell type with specific properties, most notably, the regulated secretion of insulin. It is not easy to reconstruct this regulated system outside the pancreatic beta cells, as several cellular structures and proteins are required for the secretion of insulin in response to changes in extracellular glucose levels. In this regard, liver cells may turn out to be good candidates for regulated insulin secretion, as liver cells and pancreatic beta cells are similar in terms of their expression of GLUT 2 and the glucose phosphorylation enzyme glucokinase, which comprise the key elements of the glucose-sensing system.[27] Moreover, K_{ATP} channels, which are the final effector molecules involved in insulin secretion in pancreatic beta cells, are normally expressed in liver cells.[28] However, K_{ATP} channels in primary rat hepatocytes are not affected by voltage or Ca^{2+} stimulation.[29] Thus, glucose-mediated ATP production and the subsequent reduced activity of functional K_{ATP} channels are essential for the reconstruction of a glucose-responsive system. With regard to this, Liu *et al.*[9] reported that the coexpression of insulin and GLUT 2 genes in HepG2 cells inhibits functional K_{ATP} channel currents and increases glucose-stimulated insulin secretion. We have confirmed these observations in this study. Moreover, when we employed these observations in the insulin gene therapy of STZ-induced diabetic rats, we found that diabetic Ins/G rats had improved glucose tolerance and secreted more insulin in response to glibenclamide. As a result, postprandial glucose levels were more improved in diabetic Ins/G rats.

Unlike virus-based methods to deliver genes, nonviral delivery methods are considered to be safe, cost-effective and less likely to induce immune responses. However, they are hampered by a more limited time span of transgene expression as well as lower gene transfer efficacy compared with viral vectors.[30] For example, it has been shown that while intravenous or intraportal treatment of STZ-induced diabetic rats with a nonviral vector expressing the insulin gene improved their blood glucose levels, the animals became hyperglycemic again within 1 week.[25,31] The duration of gene expression can be improved by employing the EBV-based plasmid vector in various tissues,[10,11,32,33] even though some reports showed prolonged gene expression without the EBV replicon.[34,35] With regard to insulin gene delivery into liver, recently, Yasutomi *et al.*[33] reported that hydrodynamic-based transfection of diabetic mice liver with naked EBV-based plasmid vectors containing the proinsulin gene resulted in efficient hormone production. In this study, we found that the employment of EBV replicon vector system led to prolonged expression of the transfected insulin gene and lowering blood glucose levels did not significantly differ from those of nondiabetic rats for 22 days. On the other hand, transfection of

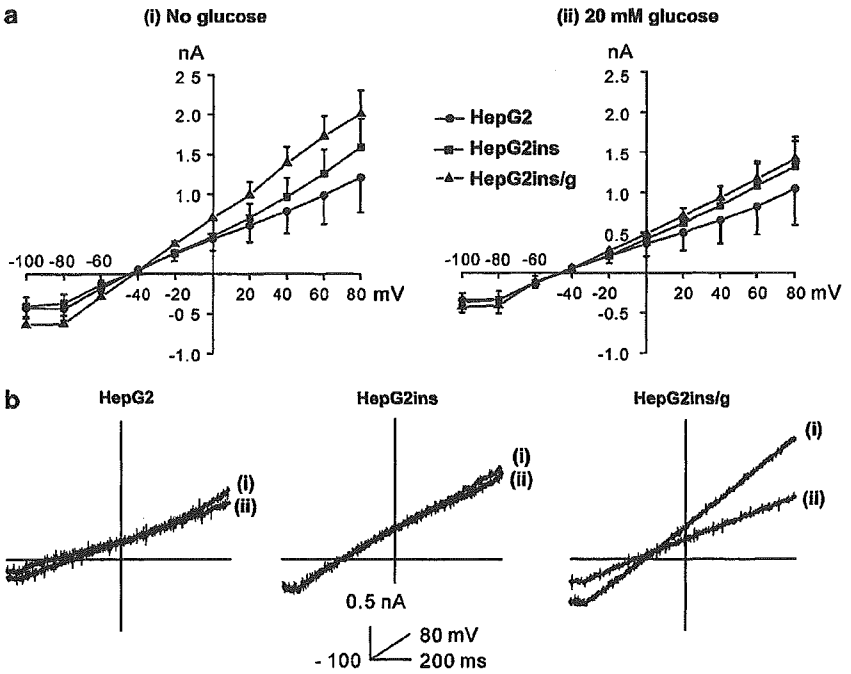

Figure 6 Effect of glucose on whole-cell currents in HepG2 cells transfected with pEBAct-ins/-glut2. (**a**) Mean current–voltage relationships in the absence of glucose (i) or the presence of 20 mM glucose (ii). Diazoxide (300 μM) was present in the bath solution on all occasions. Values shown are means±s.e.m. (n=4–6 for each trace). (**b**) Representative traces in the absence of glucose (i) or the presence of 20 mM glucose (ii) obtained by 200-ms ramp pulses from −100 to +80 mV applied at a holding potential of −50 mV. HepG2, empty-vector-transfected HepG2 cells; HepG2ins, HepG2 cells transfected with pEBAct-ins; HepG2ins/g, HepG2 cells transfected with pEBAct-ins plus pEBAct-glut2.

Table 1 Profile of parameters of liver function in the experimental animal model

	NC	*4 days (n=8 for each group)*			*22 days (n=8 for each group)*		
		STZ-C	*Ins*	*Ins/G*	*STZ-C*	*Ins*	*Ins/G*
AST	78.2±5.6	102.5±6.7*	94.9±6.7*	92.7±4.4*	145.9±9.3**	99.1±6.3#	92.5±6.9#
ALT	63.4±3.7	88.6±7.5*	91.6±5.6*	86.8±6.7*	149.7±7.9**	97.4±8.3#	93.1±9.4#
ALP	38.6±3.4	60.3±5.3*	54.1±5.7*	46.7±3.3	73.5±4.6**	53.4±3.5##	51.4±5.1##
T-Bil	0.26±0.03	0.39±0.03*	0.33±0.04	0.31±0.05	0.69±0.06**	0.42±0.03#	0.37±0.04#

Data are shown as mean±s.e.m., *P<0.05 compared with NC, **P<0.001 compared with NC, #P<0.01 compared with STZ-C (22 days), ##P<0.05 compared with STZ-C (22 days). NC=nondiabetic control rats; STZ-C=STZ-induced diabetic rats; Ins=STZ-induced diabetic rats treated with pEBAct-ins; Ins/G=STZ-induced diabetic rats treated with pEBAct-ins plus pEBACt-glut2; AST=aspartate transaminase (U/L); ALT=alanine transaminase (U/L); ALP=alkaline phosphatase (U/L); T-Bil=total bilirubin (mg/dl).

HVJ-E vector with insulin plasmids lacking EBV led to this range of fasting glucose levels only for 7 days (data not shown). It has been suggested that the EBV replicon vector may be more stable in nondividing rodent cells compared to dividing rodent cells, presumably because of its ability to be retained in the nucleus. Due to this, liver cells may be a good target for long-term expression of the insulin gene in the EBV replicon vector. The ability of the plasmid to autonomously replicate in human cell lines may be another advantage of the EBV replicon vector,[14,32] which can be useful in clinical application. However, it will be necessary to develop a technique that enables more prolonged gene expression for this method to be used in a clinical context.

We and others have reported that HVJ-liposome-mediated gene delivery is successful in transferring genes into target tissues.[12,23–25] Our previous study showed that fasting blood glucose levels in STZ-induced diabetic rats were transiently normalized by portal vein injection of HVJ-liposomes containing human insulin expression vector.[31] Alternatively, repeated intravenous administrations of the insulin vector can also result in a sustained improvement of blood glucose levels in diabetic animals without antigenecity against HVJ.[25] However, systemic administration of the insulin gene may cause gene expression in an unwanted tissue and other systemic side effects. To overcome these issues, we developed a HVJ-E vector delivery system that is even more effective than HVJ-liposomes for *in vivo* gene transfer, especially when injected directly into the liver.[26] In this study, the target gene was delivered into a surgically exposed rat liver. However, ultrasound-guided

transcutaneous liver injections have been clinically established as a relatively safe technique in human. Thus, repeated injections of the gene would also be feasible in clinical practice.

In conclusion, liver-directed gene therapy using an HVJ-E vector containing EBV plasmids resulted in a prolonged decrease in blood glucose levels in STZ-induced diabetic rats. Moreover, our data suggest that cotransfecting genes encoding insulin and the GLUT 2 transporter reconstitutes a physiologically regulated insulin secretion system in the diabetic rat liver. The present study provides a novel insulin gene therapy strategy that could be applied in clinical medicine in the future.

Materials and methods

Construction of plasmids

Furin-cleavable human preproinsulin cDNA was constructed as described previously.[18] Human GLUT 2 cDNA was purchased from Korea UniGene Information (Daejeon, Korea).

The EBV-based plasmid (pEBc) expression vector was constructed by subcloning the human insulin gene and the human GLUT 2 gene. The EBV-based plasmid contained the EBV origin of replication (*oriP*), the EBV nuclear antigen EBNA-1 and the ampicillin-resistance gene. pEBAct was constructed by replacing the cytomegalovirus promoter of pEBc with the chicken β-actin promoter derived from pAct-CAT.[36] pEBAct-ins was constructed by cloning the insulin gene into the *Bam*HI/*Xba*I site of the pEBAct plasmid. pEBAct-glut2 was constructed by cloning the GLUT 2 gene into the *Eco*RI/*Not*I site of the pEBAct plasmid. The sequences of all the cloning plasmids were confirmed by DNA sequencing. Plasmids were amplified in DH-5α cells and purified by a Qiagen plasmid Maxi kit (Qiagen, Hilden, Germany).

Primary rat hepatocyte isolation and cell culture

Primary rat hepatocytes were isolated from rat liver at 4 days after transfection. Rats were anesthetized with sodium pentobarbital (50 mg/kg body weight) and the liver of each animal was surgically exposed. The liver was first perfused with resuspension buffer (150 mM NaCl, 10 mM KCl, 1 mM $NaH_2PO_4 \cdot 2H_2O$, 0.8 mM $Na_2HPO_4 \cdot 2H_2O$, 1 mM EGTA, 0.8 mM $NaHCO_3$, 10 mM D-glucose, 10 mM HEPES, pH 7.2) at 30–50 ml/min for 5–10 min and was perfused with collagenase solution (HBSS (9.5 g/l), 0.8 mM $NaHCO_3$, 0.9 mM $CaCl_2 \cdot 2H_2O$, 10 mM HEPES, 0.5 g/l collagenase IA (Sigma, St Louis, MO, USA), 50 mg/l trypsin inhibitor, pH 7.5) at 30–50 ml/min for 5–10 min. After perfusion, the liver extract was chapped and filtered, and a pellet was obtained by centrifugation at 800 r.p.m. for 2–5 min at 4°C. The hepatocyte viability greater than 80% as detected by trypan blue was used for protein extraction.

HepG2 human hepatoma cells were grown in DMEM (Gibco-BRL, Grand Island, NY, USA) supplemented with 10% fetal bovine serum (FBS; Hyclone, Logan, UT, USA) penicillin (10 000 U/ml) and streptomycin (10 000 μg/ml) at 37°C in a 5% CO_2 humidified atmosphere.

Transfection of HepG2 cells and static stimulation of insulin secretion

HepG2 cells were maintained until reaching 60–80% confluence, after which 1×10^5 cells/well were seeded in 12-well plates and fed with 1 ml/well culture medium prior to the transfection. All transfections were carried out with LipofectAmine 2000™ reagent (Invitrogen, Carlsbad, CA, USA). The expression plasmid DNA and reagent (molar ratio; DNA:lipid = 1:3) mixtures were added to the culture plates according to the manufacturer's instructions. After transfection, the cells were incubated at 37°C for 5 h, after which culture medium with 0.5% FBS was added and the cells were cultured in a 5% CO_2 incubator for 24 h. To assess the effect of statically stimulating insulin secretion, the cells were incubated for 1 h in modified Krebs-Ringer bicarbonate buffer (114 mM NaCl, 4.4 mM KCl, 1 mM $MgSO_4$, 29.5 mM $NaHCO_3$, 1.28 mM $CaCl_2$, 0.1% BSA, 10 mM HEPES, pH 7.4), after which 5 or 25 mM glucose was added for 1 h. The supernatant was collected and the secreted insulin levels were analyzed by using a rat insulin radioimmunoassay kit (Linco Research, St Charles, MO, USA).

Recordings of single K_{ATP} channel activity

The whole-cell configuration of the conventional patch-clamp technique was used to measure the diazoxide-induced K_{ATP} current of HepG2ins, HepG2ins/g or empty-vector-transfected HepG2 cells. Patch pipettes had a resistance of 3–5 MΩ. The whole-cell currents were recorded by using an Axopatch 200B patch-clamp amplifier (Axon Instruments, Forster, CA, USA), passed onto an A/D converter (Digidata 1312; Axon) and later analyzed with Pclamp 8.2 software (Axon). Data were filtered at 5 kHz and sampled at 1 kHz.

During the experiments, single cells on a cover glass (10×2 mm) were bathed in a solution composed of (in mM) 140 Na-acetate, 1 $MgCl_2$, 1 $CaCl_2$, 10 HEPES, adjusted to pH 7.4 with NaOH. The pipette solution contained (in mM) 136 K-acetate, 4 KCl, 1 EGTA, 10 HEPES, adjusted to pH 7.3 with KOH. The experiments were performed at room temperature (20–22°C).

Diabetes induction by STZ

The 8-week-old male Sprague–Dawley rats (Hyochang, Daegu, Korea) weighing between 230 and 260 g were used. Diabetes was induced in rats by two consecutive intraperitoneal injections of STZ (80 mg/kg body weight; Sigma, St Louis, USA). Only rats with blood glucose levels above 300 mg/dl were kept in the protocol and randomized for the experiments. All procedures were in accordance with the institutional guidelines for animal research.

In vivo *gene delivery*

Diabetic rats were anesthetized with sodium pentobarbital (50 mg/kg body weight) and the liver of each animal was surgically exposed. The HVJ-E vector was donated by Ishihara Sangyo Kaisha Ltd (Osaka, Japan). The HVJ-E vector containing pEBAct-ins (100 μg) with or without pEBAct-glut2 (100 μg) was directly injected into four sites on the right lobe margin of the liver. After confirming the absence of backward flow, the rat abdomens were sutured.

IPGTT and glibenclamide stimulation test

For IPGTT and glibeclamide stimulation tests, rats were fasted for 6 h, glucose (2 g/kg of body weight) or glibenclamide (10 mg/kg of body weight) was injected intraperitoneally, and blood was drawn from the tail vein every 15 or 30 min. Blood glucose and insulin levels were then measured.

Measurement of blood glucose, plasma insulin and C-peptide, and serum AST, ALT, ALP and total bilirubin levels

Blood glucose levels were measured by glucose reagent strips and a glucometer (Abbott) or by the glucose oxidase method (Cobas integra 800, Roche, Switzerland). Plasma insulin levels were measured by using an ^{125}I-insulin double antibody rat insulin radioimmunoassay kit (Linco Research). This radioimmunoassay recognizes both proinsulin and active insulin of rat and human. C-peptide levels were measured by using a human or rat ^{125}I-C-peptide double antibody radioimmunoassay kit (Linco Research). The serum levels of AST, ALT, ALP and total bilirubin were measured in an autochemical analyzer (Hitachi 747, Tokyo, Japan) using the ultraviolet assay method.

Western blot analysis

The primary isolated hepatocytes were homogenized in IPH lysis buffer (50 mM Tris (pH 8.0), 150 mM NaCl, 5 mM EDTA, 0.5% NP-40, 100 mM PMSF, 1 M DTT, 1 mg/ml leupeptin, 1 mg/ml aprotinin). Cells were extracted at 4°C for 30 min and then centrifuged at 12 000 r.p.m. for 20 min. The supernatant was collected and served as the cell lysate. Protein quantification was determined by using a Bradford protein assay system (Biorad Laboratories, Hercules, USA). Cell lysates (30 μg/lane) were subjected to 10% SDS-PAGE electrophoresis and transferred to an Immobilon-P-transfer-membrane (Millipore, Bedford, MA, USA). The membrane was reacted with rabbit anti-GLUT-2 1:1000 (Alpha Diagnostic, San Antonio, TX, USA), followed by incubation with a horseradish peroxidase-linked secondary antibody and detection using the ECL Western blotting detection system, as specified by the manufacturer.

Histological analysis

After their transfection with the HVJ-E vector, the animals were either killed when their glucose levels became lower (day 4) or at the end of the study (day 25). Liver tissues were collected by perfusion, fixed in 4% paraformaldehyde, and embedded in paraffin. For immunohistochemistry, 4 μm thick sections were cut, incubated with mouse anti-insulin monoclonal antibody (1:300 dilution; Chemicon, CA, USA) and processed for DakoCytomation (Dako Co, CA, USA) immunohistochemistry according to the standard manual protocol.

Statistical analysis

Results are expressed as mean$\pm$s.e.m. Analysis of variance was performed with Duncan's test and used to determine significant differences in multiple comparisons. Differences were considered to be statistically significant at $P<0.05$. All experiments were performed at least three times.

Acknowledgements

This work was supported by the Grant No. RTI04-01-01 and RTI04-03-02 from the Regional Technology Innovation Program of the Ministry of Commerce, Industry and Energy (MOCIE). We thank Ishihara Sangyo Kaisha, Ltd (Osaka, Japan) for donating HVJ-E vector.

References

1 Miller AD. Human gene therapy comes of age. *Nature* 1992; **357**: 455–460.
2 Thompson L. At age 2, gene therapy enters a growth phase. *Science* 1992; **258**: 744–746.
3 Hollingsworth SJ, Barker SG. Gene therapy: into the future of surgery. *Lancet* 1999; **353** (Suppl): SI19–SI20.
4 Yoon JW, Jun HS. Recent advances in insulin gene therapy for type 1 diabetes. *Trends Mol Med* 2002; **8**: 62–68.
5 Yechoor V, Chan L. Gene therapy progress and prospects: gene therapy for diabetes mellitus. *Gene Therapy* 2004; **12**: 101–107.
6 Lee HC, Kim SJ, Kim KS, Shin HC, Yoon JW. Remission in models of type 1 diabetes by gene therapy using a single-chain insulin analogue. *Nature* 2000; **408**: 483–488.
7 Chen R, Meseck ML, Woo SL. Auto-regulated hepatic insulin gene expression in type 1 diabetic rats. *Mol Ther* 2001; **3**: 584–590.
8 Mitanchez D, Chen R, Massias JF, Porteu A, Mignon A, Bertagna X *et al.* Regulated expression of mature human insulin in the liver of transgenic mice. *FEBS Lett* 1998; **421**: 285–289.
9 Liu GJ, Simpson AM, Swan MA, Tao C, Tuch BE, Crawford RM *et al.* ATP-sensitive potassium channels induced in liver cells after transfection with insulin cDNA and the GLUT 2 transporter regulate glucose-stimulated insulin secretion. *FASEB J* 2003; **17**: 1682–1684.
10 Min KA, Oh ST, Yoon KH, Kim CK, Lee SK. Prolonged gene expression in primary porcine pancreatic cells using an Epstein–Barr virus-based episomal vector. *Biochem Biophys Res Commun* 2003; **305**: 108–115.
11 Saeki Y, Wataya-Kaneda M, Tanaka K, Kaneda Y. Sustained transgene expression *in vitro* and *in vivo* using an Epstein–Barr virus replicon vector system combined with HVJ liposomes. *Gene Therapy* 1998; **5**: 1031–1037.
12 Tsujie M, Isaka Y, Nakamura H, Kaneda Y, Imai E, Hori M. Prolonged transgene expression in glomeruli using an EBV replicon vector system combined with HVJ liposomes. *Kidney Int* 2001; **59**: 1390–1396.
13 Lupton S, Levine AJ. Mapping genetic elements of Epstein–Barr virus that facilitate extrachromosomal persistence of Epstein–Barr virus-derived plasmids in human cells. *Mol Cell Biol* 1985; **5**: 2533–2542.
14 Yates JL, Warren N, Sugden B. Stable replication of plasmids derived from Epstein–Barr virus in various mammalian cells. *Nature* 1985; **313**: 812–815.
15 Wu H, Kapoor P, Frappier L. Separation of the DNA replication, segregation, transcriptional activation functions of Epstein–Barr nuclear antigen 1. *J Virol* 2002; **76**: 2480–2490.
16 Ilan Y, Saito H, Thummala NR, Chowdhury NR. Adenovirus-mediated gene therapy of liver diseases. *Semin Liver Dis* 1999; **19**: 49–59.
17 Muruve DA, Barnes MJ, Stillman IE, Libermann TA. Adenoviral gene therapy leads to rapid induction of multiple chemokines and acute neutrophil-dependent hepatic injury *in vivo*. *Hum Gene Ther* 1999; **10**: 965–976.
18 Park YM, Woo S, Lee GT, Ko JY, Lee Y, Zhao ZS *et al.* Safety and efficacy of adeno-associated viral vector-mediated insulin gene transfer via portal vein to the livers of streptozotocin-induced diabetic Sprague–Dawley rats. *J Gene Med* 2005; **7**: 621–629.

19 Kay MA, Glorioso JC, Naldini L. Viral vectors for gene therapy: the art of turning infectious agents into vehicles of therapeutics. *Nat Med* 2001; **7**: 33–40.
20 Russell DW, Kay MA. Adeno-associated virus vectors and haematology. *Blood* 1999; **94**: 864–874.
21 Mulligan RC. The basic science of gene therapy. *Science* 1993; **260**: 926–932.
22 Dzau VJ, Mann MJ, Morishita R, Kaneda Y. Fusigenic viral liposome for gene therapy in cardiovascular diseases. *Proc Natl Acad Sci USA* 1996; **93**: 11421–11425.
23 Ahn JD, Morishita R, Kaneda Y, Kim HS, Chang YC, Lee KU *et al.* Novel E2F decoy oligodeoxynucleotides inhibit *in vitro* vascular smooth muscle cell proliferation and *in vivo* neointimal hyperplasia. *Gene Therapy* 2002; **9**: 1682–1692.
24 Ahn JD, Morishita R, Kaneda Y, Kim HJ, Kim YD, Lee HJ *et al.* Transcription factor decoy for AP-1 reduces mesangial cell proliferation and extracellular matrix production *in vitro* and *in vivo*. *Gene Therapy* 2004; **11**: 916–923.
25 Morishita R, Gibbons GH, Kaneda Y, Ogihara T, Dzau VJ. Systemic administration of HVJ viral coat-liposome complex containing human insulin vector decreases glucose level in diabetic mouse: a model of gene therapy. *Biochem Biophys Res Commun* 2000; **273**: 666–674.
26 Kaneda Y, Nakajima T, Nishikawa T, Yamamoto S, Ikegami H, Suzuki N *et al.* Hemagglutinating virus of Japan (HVJ) envelope vector as a versatile gene delivery system. *Mol Ther* 2002; **6**: 219–226.
27 Burcelin R, Dolci W, Thorens B. Glucose sensing by the hepatoportal sensor is GLUT2-dependent: *in vivo* analysis in GLUT2-null mice. *Diabetes* 2000; **49**: 1643–1648.
28 Malhi H, Irani AN, Rajvanshi P, Suadicani SO, Spray DC, McDoland TV *et al.* K_{ATP} channels regulate mitogenically induced proliferation in primary rat hepatocytes and human liver cell lines. Implications for liver growth control and potential therapeutic targeting. *J Biol Chem* 2000; **275**: 26050–26057.
29 Henderson RM, Graf J, Boyer JL. Inward-rectifying potassium channels in rat hepatocytes. *Am J Physiol* 1989; **171**: G1028–G1035.
30 Nishikawa M, Huang L. Nonviral vectors in the new millennium: delivery barriers in gene transfer. *Hum Gene Ther* 2001; **12**: 861–870.
31 Kaneda Y, Iwai K, Uchida T. Introduction and expression of the human insulin gene in adult rat liver. *J Biol Chem* 1989; **264**: 12126–12129.
32 Calos MP. The potential of extrachromosomal replicating vectors for gene therapy. *Trends Genet* 1996; **12**: 463–466.
33 Yasutomi K, Itokawa Y, Asada H, Kishida T, Cui FD, Ohashi S *et al.* Intravascular insulin gene delivery as potential therapeutic intervention in diabetes mellitus. *Biochem Biophys Res Commun* 2003; **310**: 897–903.
34 Chen ZY, Yant SR, He CY, Meuse L, Shen S. Linear DNAs concatemerize *in vivo* and result in sustained transgene expression in mouse liver. *Mol Ther* 2001; **3**: 403–410.
35 Chen ZY, He CY, Ehrhardt A, Kay MA. Minicircle DNA vectors devoid of bacterial DNA result in persistent and high-level transgene expression *in vivo*. *Mol Ther* 2003; **8**: 495–500.
36 Fregien N, Davidson N. Activating elements in the promoter region of the chicken beta-actin gene. *Gene* 1986; **48**: 1–11.

Available online at www.sciencedirect.com
SCIENCE DIRECT®
ELSEVIER
Biochemical and Biophysical Research Communications 334 (2005) 1121–1126
BBRC
www.elsevier.com/locate/ybbrc

Magnetic nanoparticles with surface modification enhanced gene delivery of HVJ-E vector

Norio Morishita [a,b], Hironori Nakagami [c,*], Ryuichi Morishita [b], Shin-ichi Takeda [d], Fumihito Mishima [d], BungoTerazono [d], Shigehiro Nishijima [d], Yasufumi Kaneda [c], Noriaki Tanaka [a]

[a] *Department of Gastroenterological Surgery, Transplant, and Surgical Oncology, Graduate School of Medicine and Dentistry, Okayama University, Okayama, Japan*
[b] *Division of Clinical Gene Therapy, Graduate School of Medicine, Osaka University, Osaka 565-0871, Japan*
[c] *Division of Gene Therapy Science, Graduate School of Medicine, Osaka University, Osaka 565-0871, Japan*
[d] *Division of Sustainable Energy and Environmental Engineering, Graduate School of Engineering, Osaka University, Osaka 565-0871, Japan*

Received 24 June 2005
Available online 14 July 2005

Abstract

To enter the realm of human gene therapy, a novel drug delivery system is required for efficient delivery of small molecules with high safety for clinical usage. We have developed a unique vector "HVJ-E (hemagglutinating virus of Japan-envelope)" that can rapidly transfer plasmid DNA, oligonucleotide, and protein into cells by cell-fusion. In this study, we associated HVJ-E with magnetic nanoparticles, which can potentially enhance its transfection efficiency in the presence of a magnetic force. Magnetic nanoparticles, such as maghemite, with an average size of 29 nm, can be regulated by a magnetic force and basically consist of oxidized Fe which is commonly used as a supplement for the treatment of anemia. A mixture of magnetite particles with protamine sulfate, which gives a cationic surface charge on the maghemite particles, significantly enhanced the transfection efficiency in an in vitro cell culture system based on HVJ-E technology, resulting in a reduction in the required titer of HVJ. Addition of magnetic nanoparticles would enhance the association of HVJ-E with the cell membrane with a magnetic force. However, maghemite particles surface-coated with heparin, but not protamine sulfate, enhanced the transfection efficiency in the analysis of direct injection into the mouse liver in an in vivo model. The size and surface chemistry of magnetic particles could be tailored accordingly to meet specific demands of physical and biological characteristics. Overall, magnetic nanoparticles with different surface modifications can enhance HVJ-E-based gene transfer by modification of the size or charge, which could potentially help to overcome fundamental limitations to gene therapy in vivo.

Keywords: Magnetic nanoparticle; HVJ-E; Drug delivery system; Gene therapy

Progress in gene therapy requires a novel drug delivery system (DDS). To enhance the transfection efficiency, we developed a hybrid vector utilizing the envelop of HVJ (hemagglutinating virus of Japan). The HVJ-E vector rapidly transfers plasmid DNA, oligonucleotide or protein into cells by cell fusion [1]. However, this modality of targeting is still insufficient for rapid and specific accumulation of active vectors in target tissues. One solution is to engineer the surface proteins of viral vectors or to couple targeting ligands to viral as well as non-viral vectors, which might further improve tissue selectivity [2–5]. Thus, we examined modification of the membrane surface of HVJ to achieve an improvement.

In this study, we focused on magnetic nanoparticles, such as magnetite and maghemite, with an average size

* Corresponding author. Fax: +81 6 6879 3909.
E-mail address. nakagami@gts.med.osaka-u.ac.jp (H. Nakagami).

0006-291X/$ - see front matter © 2005 Elsevier Inc. All rights reserved.
doi:10.1016/j.bbrc.2005.06.204

from 20 to 50 nm, which can be positionally regulated by a magnetic force. Magnetic nanoparticles basically consist of oxidized Fe, which is commonly used as a supplement for the treatment of anemia. We hypothesized that the association of magnetite and HVJ-E technology could allow the rapid attachment of HVJ-E and cells by application of a magnetic force, leading to enhanced transfection efficiency. Moreover, magnetic nanoparticles can be modified with several chemical compounds to allow modification of the charge, size, and affinity. In addition, there is increasing interest in using magnetic resonance imaging (MRI) to monitor the in vivo behavior of proteins labeled with magnetic nanoparticles [6,7]. Indeed, magnetic nanoparticles were recently used for gene transfection, because magnetic targeting exploits paramagnetic particles as drug carriers, guiding their accumulation in target tissues with strong local magnetic fields [8,9]. Here, the present study demonstrated that modification of magnetic nanoparticles with protamine sulfate or heparin enhanced the transfection efficiency associated with HVJ-E system in cultured cells in vitro and in murine liver in vivo.

Materials and methods

Preparation of HVJ-E vector and plasmid DNA. HVJ-E vector was obtained from Ishihara (Osaka, Japan). Basically, aliquots of the inactivated virus (6 AU) were suspended in 40 μl TE solution (10 mM Tris–Cl, pH 8.0, 1 mM EDTA) and mixed with plasmid DNA (30 μg), and 0.3% Triton X. The mixture was centrifuged at 18,500*g* for 15 min at 4 °C. After washing the pellet with 1 ml balanced salt solution (BSS; 10 mM Tris–Cl, pH 7.5, 137 mM NaCl, and 5.4 mM KCl) to remove the detergent and unincorporated DNA, the envelop vector was suspended in 300 μl BSS. The titer of the inactivated virus was modified according to each experiment. pEGFP-C1 was purchased from Clontech (CA, USA). pCMV-luciferase-GL2 or GL3 was constructed by cloning the luciferase gene from the pGL2 (for in vitro culture) or pGL3 (for in vivo experiment)-promoter vector (Promega, Madison, WI, USA) into pcDNA3 (5.4 kb) (Invitrogen, San Diego, CA, USA). Plasmids were purified with a Qiagen plasmid isolation kit (Hilden, Germany). FITC-oligodeoxynucleotides (ODN) (random sequence) were purchased from Gene Design (Osaka, Japan).

Preparation of magnetic HVJ-E vector. Commercially available maghemite particle (NanoTek γ-Fe_{23}, C.I. KASEI) was used for the preparation of magnetic HVJ-E vector and plasmid DNA in the present study. The averaged primary size of maghemite particle used in this study was 29 nm. The particles were mixed with protamine sulfate or haparin solution to prepare magnetic nanoparticles modified with bio-polymers, which consist of cationic polymer adsorbed with ferromagnetic nano-sized particles. The prepared magnetic nanoparticles were then mixed with HVJ-E vector to provide ferromagnetism to the HVJ-E vector.

Measurement of zeta potential of maghemite particles. Zeta potential is an important parameter in understanding electrostatic colloidal dispersion stability. Zeta potential is the charge that a particle acquires in a particular medium. It is dependent upon the pH, ionic strength and concentration of a particular component. The mobility of particles undergoing electrophoresis is measured by the technique of laser Doppler electrophoresis. This measured electrophoretic mobility is then converted to zeta potential using established theories. In order to know the surface property of the magnetic vector, the zeta potential of the particles with and without surface modification was determined using a capillary cell electrophoresis technique (Zetasizer Nano ZS, Malvern, UK). Mixtures of magnetite particles with and without surface modification with protamine sulfate or heparin and the prepared magnetic HVJ-E vector and plasmid DNA were used.

Gene transfer in vitro and in vivo. For in vitro transfection, 5×10^5 cells were prepared in 6-well culture dishes at 1 day before transfection. HVJ-E vector (1 or 0.2 AU) containing luciferase plasmid (GL2: 5 or 1 μg) or FITC-ODN (2 or 0.4 μg) was mixed with various concentrations of magnetite and DMEM containing 10% FCS, and added to cells cultured in DMEM supplemented with 10% FBS on a magnetic sheet. The magnetic sheet was placed under the 6-well culture dish. The magnetic field gradient is one of the parameters affecting the strength of the magnetic force applied to the magnetic vectors to sediment to the cell surface. Magnetic field measurements were performed by Hall detector to calculate the magnetic field gradient. A 3-axis Hall effect teslameter (MetroLab THM 7025, METROLAB Instruments SA, Switzerland) was used to measure the magnetic field. The averaged value of the measured magnetic field at the sheet surface was approximately 1.2 mT and the calculated value of the field gradient was 1.7 mT/cm. After 10 min of incubation at 37 °C under 5% CO_2, the medium was replaced and the cells were cultured overnight before examination of gene expression. GFP expression or FITC ODN-transfected cells were observed under a fluorescence microscope.

For in vivo transfection, HVJ-E vector (2 AU) containing luciferase gene or GFP (10 μg) suspended in 100 μl PBS was injected directly into the liver of BALB/c mice (8 weeks of age; $n = 5$–9) with several kinds of magnetite. All animals were handled in a humane manner in accordance with the guidelines of the Animal Committee of Osaka University. Frozen sections of liver were stained with hematoxylin or immunostained with anti-GFP antibody (Molecular Probes, Eugene, OR).

Luciferase activity and LDH release. Luciferase activity was measured following the manufacturer's instructions (Promega Madison) [10]. Twenty-four hours after transfection, cells were washed once with PBS and then incubated with lysis buffer. The protein concentration was determined using the Bio-Rad protein assay adapted for use in a 96-well plate. After 20 μl cell extract was mixed with 100 μl luciferase assay reagent (Promega, Madison), the light produced was measured for 2 s using a luminometer.

The extent of cell death was assessed using a commercially available kit (Wako, Osaka) to measure released LDH activity from dead cells according to previous reports [11,12], because loss of cell membrane integrity was observed in both necrotic and apoptotic cells. The percentage of LDH release was calculated relative to the maximum cell death of cells treated with 1% Triton X-100 for 10 min.

Electronmicroscopy. Electron microscopic observation was performed as previously described [1]. After mixing HVJ-E vector and PS-coated magnetite, they were fixed at 4 °C with 1% glutaraldehyde for 2 h and washed twice with 0.1 M phosphate buffer, 10% sucrose. They were further fixed with 1% osmium tetroxide for 30 min and washed twice with 0.1 M phosphate buffer 10% sucrose, and dehydrated through a graded ethanol series (70–100%) and propylene oxide. They were then embedded in epoxy resin (Quetol 812). For transmission electron microscopic (TEM) observation, ultrathin sections were obtained with an ultramicrotome, stained doubly with uranyl acetate and lead citrate, and observed under an electron microscope (H-7100 Hitachi) at an accelerating voltage of 75 kV.

Statistical analysis All values are expressed as means ± SEM. Analysis of variance with subsequent Bonferroni's/Dunnet's test was employed to determine the significance of differences in multiple comparisons. Values of $P < 0.05$ were considered statistically significant.

Results

Basic characteristics of magnetic nanoparticle, maghemite

To evaluate the HVJ-E vector system mixed with maghemite, we measured luciferase activity to evaluate

transfection activity and LDH release to evaluate cell toxicity after transfection. We mixed several doses of maghemite (from 100 ng/ml to 1 mg/ml) with HVJ-E vector infusing luciferase plasmid. However, unexpectedly, we did not find any improvement in transfection efficiency as assessed by luciferase activity in BHK-21

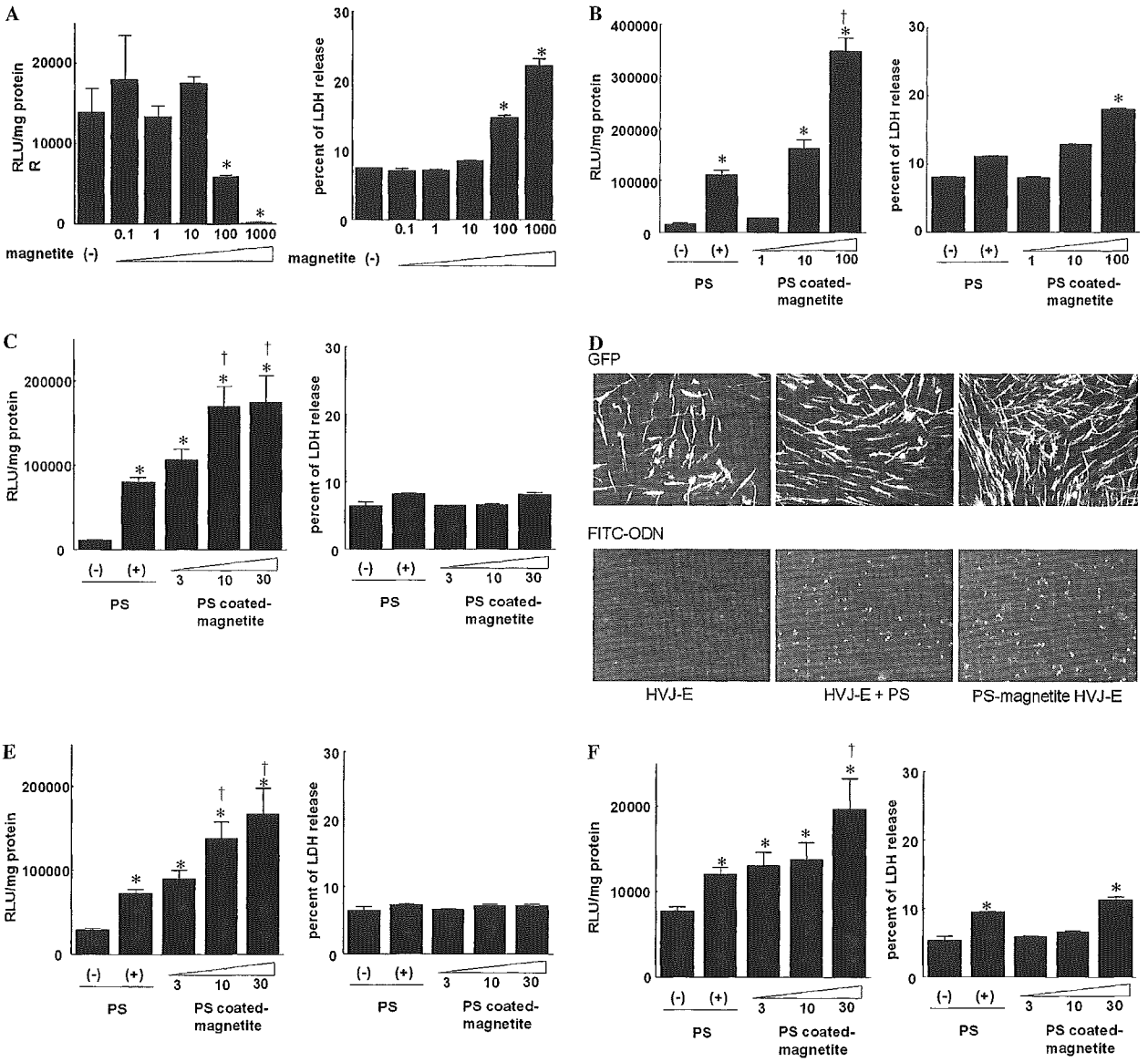

Fig. 1. Transfection efficiency (luciferase activity) and cell toxicity (LDH release) of maghemite-associated HVJ-E vector. (A) HVJ-E vector (1 AU) containing the luciferase expression plasmid (5 μg) was transferred to BHK-21 cells seeded in 6-well dishes with various concentrations of non-coated maghemite and incubated for 10 min. The final concentrations of maghemite were as follows: 0, 0.1, 1, 10, 100, and 1000 μg/ml non-coated maghemite. $^{*}P < 0.01$ vs. magnetite (−). (B) HVJ-E vector (1 HAU) containing the luciferase expression plasmid (5 μg) was transferred to BHK-21 cells seeded in 6-well dishes with various concentrations of protamine sulfate-coated maghemite and incubated for 10 min. The final concentrations of PS and PS-coated maghemite were as follows: 100 μg/ml PS, 1, 10, and 100 μg/ml PS-coated maghemite. (C) HAU HVJ-E vector (0.2 HAU) containing the luciferase expression plasmid (1 μg) was transferred to BHK-21 cells with various concentrations of magnetite and incubated for 10 min. The final concentrations of PS and PS-coated maghemite were as follows; 100 μg/ml PS, 3, 10, and 30 μg/ml PS-coated maghemite. Luciferase gene expression was examined 24 h after transfer. Results are shown as means + SE. $^{*}P < 0.01$ vs. PS(−), $^{\dagger}P < 0.01$ vs. PS(+). (D) Representative example of BHK-21 cells transfected with the EGFP plasmid (1 μg) or FITC-ODN (1 μg) using PS-coated maghemite (30 μg/ml) with HVJ-E vector (0.2 AU) under fluoromicroscopy. Upper panels show EGFP overexpressing cells and lower panels show FITC ODN-overexpressing cells (magnification 100×). (E,F) HVJ-E vector (0.2 AU) containing luciferase expression plasmid was transferred to (E) COS7 and (F) Bovine aortic endothelial cells seeded in 6-well dished with various concentrations of maghemites and incubated for 10 min. The final concentration of PS or PS-coated maghemite are as follows: 100 μg/ml PS, 3, 10, and 30 μg/ml PS-coated maghemite. Luciferase gene expression was examined 24 h after transfer. Results are shown as means − SE. $^{*}P < 0.01$ vs. PS(−), $^{\dagger}P < 0.01$ vs. PS(+).

cells, whereas a high dose of maghemite induced cell death as assessed by LDH release (Fig. 1A). From these results, we speculated that there might be a close association, such as electrostatic interaction, between HVJ-E and maghemite. Since we have previously reported that protamine sulfate (PS), a low-molecular-weight naturally polycationic peptide (~4000 Da), enhanced the transfection efficiency based on the HVJ-E vector in an in vitro culture system [1], we coated the surface of maghemite with PS. After modification with PS, the zeta potential of maghemite was changed to 23.8 ± 1.8 mV from 17.5 ± 1.6 mV, which suggests that surface coating of maghemite enhanced its cationic charge. Interestingly, a mixture of PS-coated maghemite with HVJ-E vector significantly enhanced the transfection efficiency in a dose-dependent manner (Fig. 1B, $P < 0.01$). However, induction of cell death was still detected at a high dosage. To avoid cell toxicity, we reduced the PS-coated maghemite dose and titer of HVJ-E. Finally, we found a suitable dose of PS-coated maghemite (30 μg/ml) and HVJ-E titer (0.2 AU) for BHK cells (Fig. 1C). Using this combination, addition of PS-coated maghemite to the HVJ-E vector significantly enhanced transfection efficiency without apparent cell toxicity (Fig. 1C, $P < 0.01$). Using the same system, high transfection efficiency into BHK cells was also achieved using EGFP gene or FITC-oligodeoxynucleotide (Fig. 1D). We also examined the transfection efficacy of this novel vector system in COS7 cells and bovine aortic endothelial cells. Although the absolute values of transfection efficiency were different in each cell type, high transfection efficiency could be obtained using the luciferase gene in COS7 cells without apparent cell toxicity (Fig. 1E, $P < 0.01$). Similarly, in bovine aortic endothelial cells, a mixture of PS-coated magnetite with the HVJ-E vector significantly enhanced the transfection efficiency in a dose-dependent manner (Fig. 1F, $P < 0.01$). However, in bovine aortic endothelial cells, treatment with PS (100 ng/ml) or high-dose PS-coated maghemite (30 μg/ml) induced cell toxicity assessed by LDH release. Thus, the optimum

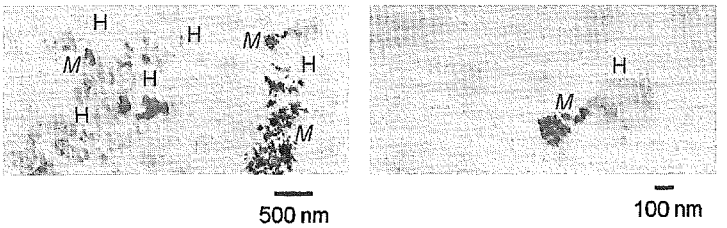

Fig. 2. Representative transmission electron microscopic (TEM) views showing co-existence of HVJ-E vector and PS-coated maghemite: H, HVJ-E vector; M, PS-coated maghemite. Bar = 500 nm in the left panel, and 100 nm in the right panel.

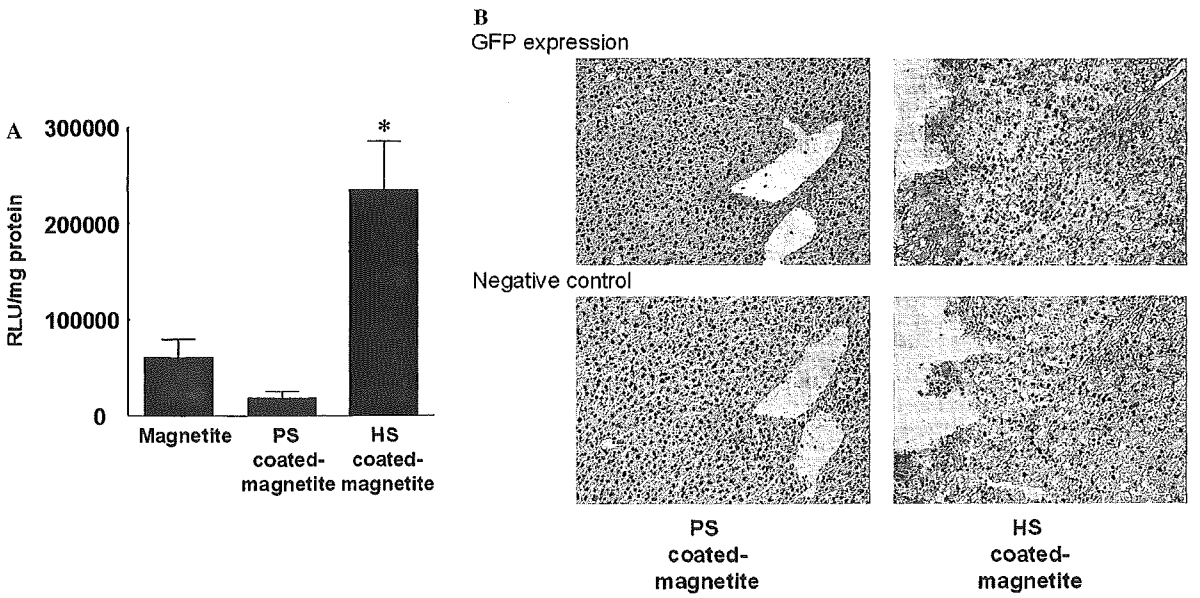

Fig. 3. Transfection efficiency (luciferase activity or EGFP expression) of protamine sulfate (PS)- or heparin sulfate (HS)-coated maghemite with HVJ-E vector. HVJ-E vector (2 AU) containing luciferase (A) or EGFP (B) was injected into the liver with non-coated maghemite, 30 μg/ml PS-coated maghemite, or 30 μg/ml heparin sulfate-coated maghemite.

Table 1
Serum AST, ALT, and LDH levels with each type of transfection

	AST (U/L)	ALT (U/L)	LDH (IU)
HVJ-E only	266 ± 32	205 ± 43	804 ± 79
HVJ-E-PS-coated magnetite	411 ± 95	147 ± 21	1113 ± 166
HVJ-E-HS-coated magnetite	297 ± 45	161 ± 91	803 ± 55

PS, protamine sulfate; HS, heparin sulfate.

dose of magnetic particles should be evaluated in each cell type.

To confirm the interaction of magnetite and the HVJ-E vector, we performed electron microscopy. PS-coated maghemite and the HVJ-E vector co-existed even though a number of maghemite particles were aggregated around the HVJ-E vector (Fig. 2).

To explore transfection in vivo, we further evaluated the maghemite-attached HVJ-E vector by direct injection into mouse liver. Unexpectedly, a mixture of maghemite surface-coated with PS did not enhance the transfection efficiency in the analysis of luciferase activity, differing from the in vitro system. Since co-treatment with heparin has been reported to enhance the transfection efficiency of the HVJ-E vector in brain tissue [13], we next coated the surface of maghemite with heparin, which might antagonize the function of PS. The zeta potential of maghemite was changed to -10.1 ± 2.3 mV from 17.5 ± 1.6 mV, which suggests that the surface coating of maghemite was changed to a fairly negative net charge. A mixture of heparin-coated maghemite with HVJ-E vector significantly enhanced the transfection efficiency in the liver (Fig. 3A, $P < 0.01$). In contrast, in BHK-21 cells, a mixture of heparin-coated maghemite with HVJ-E vector did not increase the luciferase activity (data not shown). These data suggest that suitable modifications for gene transfection differ between in vitro and in vivo. Analysis of EGFP expression in the liver by immunostaining, also confirmed marked expression obtained with heparin-coated maghemite with HVJ-E vector containing the EGFP gene as compared to PS-coated maghemite (Fig. 3B). For safety evaluation, the serum levels of AST and ALT were not further elevated in the heparin-coated maghemite group compared to the control group (Table 1). Furthermore, we tried to enhance the transfection efficiency under the influence of a magnetic field by placing a magnet on the surface of the liver. However, no obvious improvement in luciferase activity in the liver was observed (data not shown). Probably, a stronger magnetic field or more accurate control of magnetite might be necessary to enhance it.

Discussion

In this study, we demonstrated that magnetic nanoparticles with different surface modifications enhanced HVJ-E-based gene transfer by modification of the surface charge. The fundamental principle of magnetically enhanced transfection is simple and comprises the steps of formulating a magnetic vector as described above, adding it to the medium covering cultured cells or injecting it locally into a target tissue, and in addition applying a magnetic field in order to direct the vector towards the target cells. Interestingly, PS as the coating material of nanoparticles was suitable in an in vitro cell culture system, whereas heparin was suitable for gene transfer into the mouse liver in vivo.

Recently, Plank et al. proposed a new method, magnetofection, which comprised the association of vectors with superparamagnetic iron oxide nanoparticles under the application of a magnetic field [8,14]. In this system, the gene carrier itself represents a hybrid system characterized by an iron oxide inner core and a coat consisting of the cationic polymer, polyethyleminine (PEI). Using this system, the cellular uptake by magnetofection proceeds obviously by endocytosis. Interestingly, PEI might also assist the endosomal escape of a gene after transfection into cells. In contrast, in our system, transfection was mediated by a cell fusion process of the HVJ-E vector, which did not require endosomal escape, was not by endocytosis. Thus, we selected PS as the coating material of maghemite in combination with the HVJ-E system, as PS is a low-molecular-weight polycationic peptide (~4000 Da) that is FDA approved as an antidote to heparin anticoagulation [15,16]. Since both the surface of HVJ-E and the cell membrane have a negative net charge, cationic charged PS-coated maghemite can be speculated to enhance the association of HVJ-E with the cell membrane. Thus, PS-coated maghemite would actively carry HVJ-E to cultured cells under a magnetic force.

However, in an in vivo system, heparin, but not PS, was suitable as the coating material in combination with the HVJ-E vector consistent with a previous in vivo report [13] [17]. Of special interest regarding this result was a previous report showing that co-infusion of trophic factors and heparin into the rat brain significantly enhanced the volume of distribution [18]. Thus, we speculate that the distribution of these vectors may be a key to explaining this discrepancy between in vitro and in vivo gene transfer. In addition, no immunohistochemical data has been presented on potential toxic effects of heparin. The size and surface chemistry of magnetic particles could be tailored accordingly to meet specific demands of physical and biological characteristics.

Magnetically targeted drug delivery by particulate carriers to a localized disease site may be efficient as drugs, and very high concentrations of chemotherapeutic or radiological agent can be achieved near the target site, such as a tumor, without any toxic effects on normal surrounding tissue or the whole body. Magnetic carriers receive their magnetic responsiveness to a

magnetic field from incorporated materials such as magnetite, iron, nickel, cobalt, neodymium–iron–boron or samarium–cobalt. As for biomedical applications, magnetic carriers must be water-based, biocompatible, non-toxic, and non-immunogenic. The first medical application directly applied magnetite or iron powder. The first clinical cancer therapy trial was performed in Germany for the treatment of advanced solid cancer in 14 patients using magnetic microspheres that were about 100 nm in diameter and filled with 4′-epidoxorubicin [19]. The phase I study clearly showed low toxicity of the method and accumulation of MMS in the target area. However, MRI measurements indicated that more than 50% of MMS ended up in the liver [20]. Conceptually, magnetic targeting is a very promising approach. However, there are a number of physical, magnetism-related properties which require careful attention. First, more responsive magnetic materials with defined and homogenous material properties in a stable and defined oxidation state need to be synthesized. Second, the size must be small enough that they do not clog the blood vessels through which they are guided to the target organ. Third, altering the surface of magnetite with appropriate molecules should be considered, to either increase or decrease the interaction of magnetite with tissues or organs. Fourth, the magnetite size must be uniform enough to provide an equal probability of magnetic capture for each magnetite particle. Finally, the fate of the particles in the body is an important consideration both for local and systemic short- and long-term toxicity. Thus, further improvements of this hybrid vector are required in future studies.

Overall, we have developed a novel hybrid vector of HVJ-E and magnetic nanoparticles with different surface modifications in an in vitro culture system as well as in vivo. Further modification of this system with MRI might provide new therapeutic potential to achieve tissue targeting.

Acknowledgments

We thank Koichi Mori (Anges MG. Inc.), Naho Suzuki (Genomidea, Inc.), and Naoko Saito (Osaka University) for their excellent technical assistance. This work was partially supported by a Grant-in-Aid from the Organization for Pharmaceutical Safety and Research, a Grant-in-Aid from The Ministry of Public Health and Welfare, a Grant-in-Aid from Japan Promotion of Science, and The Ministry of Education, Culture, Sports, Science and Technology, the Japanese Government.

References

[1] Y. Kaneda, T. Nakajima, T. Nishikawa, S. Yamamoto, H. Ikegami, N. Suzuki, H. Nakamura, R. Morishita, H. Kotani, Mol. Ther. 6 (2002) 219–226.
[2] A.M. Haines, A.S. Irvine, A. Mountain, J. Charlesworth, N.A. Farrow, R.D. Husain, H. Hyde, H. Ketteringham, R.H. McDermott, A.F. Mulcahy, T.L. Mustoe, S.C. Reid, M. Rouquette, J.C. Shaw, D.R. Thatcher, J.H. Welsh, D.E. Williams, W. Zauner, R.O. Phillips, Gene Ther. 8 (2001) 99–110.
[3] S. Gottschalk, J.T. Sparrow, J. Hauer, M.P. Mims, F.E. Leland, S.L. Woo, L.C. Smith, Gene Ther. 3 (1996) 48–57.
[4] Y. Taniyama, K. Tachibana, K. Hiraoka, T. Namba, K. Yamasaki, N. Hashiya, M. Aoki, T. Ogihara, K. Yasufumi, R. Morishita, Circulation 105 (2002) 1233–1239.
[5] N. Tomita, R. Morishita, K. Yamamoto, J. Higaki, V.J. Dzau, T. Ogihara, Y. Kaneda, J. Gene Med. 4 (2002) 527–535.
[6] A.S. Arbab, G.T. Yocum, H. Kalish, E.K. Jordan, S.A. Anderson, A.Y. Khakoo, E.J. Read, J.A. Frank, Blood 104 (2004) 1217–1223.
[7] J.W. Bulte, T. Douglas, B. Witwer, S.C. Zhang, E. Strable, B.K. Lewis, H. Zywicke, B. Miller, P. van Gelderen, B.M. Moskowitz, I.D. Duncan, J.A. Frank, Nat. Biotechnol. 19 (2001) 1141–1147.
[8] F. Scherer, M. Anton, U. Schillinger, J. Henke, C. Bergemann, A. Kruger, B. Gansbacher, C. Plank, Gene Ther. 9 (2002) 102–109.
[9] S. Huth, J. Lausier, S.W. Gersting, C. Rudolph, C. Plank, U. Welsch, J. Rosenecker, J. Gene Med. 6 (2004) 923–936.
[10] H. Mima, R. Tomoshige, T. Kanamori, Y. Tabata, S. Yamamoto, S. Ito, K. Tamai, Y. Kaneda, J. Gene Med. 7 (2005) 888–897.
[11] S. Shimizu, Y. Eguchi, W. Kamiike, H. Matsuda, Y. Tsujimoto, Oncogene 12 (1996) 2251–2257.
[12] H. Nakagami, R. Morishita, K. Yamamoto, S.I. Yoshimura, Y. Taniyama, M. Aoki, H. Matsubara, S. Kim, Y. Kaneda, T. Ogihara, Diabetes 50 (2001) 1472–1481.
[13] M. Shimamura, R. Morishita, M. Endoh, K. Oshima, M. Aoki, S. Waguri, Y. Uchiyama, Y. Kaneda, Biochem. Biophys. Res. Commun. 300 (2003) 464–471.
[14] C. Plank, U. Schillinger, F. Scherer, C. Bergemann, J.S. Remy, F. Krotz, M. Anton, J. Lausier, J. Rosenecker, Biol. Chem. 384 (2003) 737–747.
[15] B.S. Bull, W.M. Huse, F.S. Brauer, R.A. Korpman, J. Thorac. Cardiovasc. Surg. 69 (1975) 685–689.
[16] A.S. Gervin, Surg. Gynecol. Obstet. 140 (1975) 789–796.
[17] M.Y. Mastakov, K. Baer, R.M. Kotin, M.J. During, Mol. Ther. 5 (2002) 371–380.
[18] J.F. Hamilton, P.F. Morrison, M.Y. Chen, J. Harvey-White, R.S. Pernaute, H. Phillips, E. Oldfield, K.S. Bankiewicz, Exp. Neurol. 168 (2001) 155–161.
[19] A.S. Lubbe, C. Bergemann, H. Riess, F. Schriever, P. Reichardt, K. Possinger, M. Matthias, B. Dorken, F. Herrmann, R. Gurtler, P. Hohenberger, N. Haas, R. Sohr, B. Sander, A.J. Lemke, D. Ohlendorf, W. Huhnt, D. Huhn, Cancer Res. 56 (1996) 4686–4693.
[20] A.S. Lubbe, C. Bergemann, W. Huhnt, T. Fricke, H. Riess, J.W. Brock, D. Huhn, Cancer Res. 56 (1996) 4694–4701.

J. Biomater. Sci. Polymer Edn, Vol. 16, No. 11, pp. 1447–1461 (2005)

Also available online - www.vsppub.com

Preparation of poly(ethylene glycol)-introduced cationized gelatin as a non-viral gene carrier

TOSHIHIRO KUSHIBIKI and YASUHIKO TABATA *

Department of Biomaterials, Institute for Frontier Medical Sciences, Kyoto University, 53 Kawara-cho Shogoin, Sakyo-ku, Kyoto 606-8507, Japan

Received 22 October 2004; accepted 16 April 2005

Abstract—The objective of this study was to prepare cationized gelatins grafted with poly(ethylene glycol) (PEG) (PEG-cationized gelatin) and evaluate the *in vivo* efficiency as a non-viral gene carrier. Cationized gelatin was prepared by chemical introduction of ethylenediamine to the carboxyl groups of gelatin. PEG with one terminal of active ester group was coupled to the amino groups of cationized gelatin to prepare PEG-cationized gelatins. Electrophoretic experiments revealed that the PEG-cationized gelatin with low PEGylation degrees was complexed with a plasmid DNA of luciferase, in remarked contrast to that with high PEGylation degrees. When the plasmid DNA complexed with the cationized gelatin or PEG-cationized gelatin was mixed with deoxyribonuclease I (DNase I) in solution to evaluate the resistance to enzymatic degradation, stronger protection effect of the PEG-cationized gelatin was observed than that of the cationized gelatin. The complex of plasmid DNA and PEG-cationized gelatin had an apparent molecular size of about 300 nm and almost zero surface charge. These findings indicate that the PEG-cationized gelatin–plasmid DNA complex has a nano-order structure where the plasmid DNA is covered with PEG molecules. When the PEG-cationized gelatin–plasmid DNA complex was intramuscularly injected, the level of gene expression was significantly increased compared with the injection of plasmid DNA solution. It is concluded that the PEG-cationized gelatin was a promising non-viral gene carrier to enhance gene expression *in vivo*.

Key words: Poly(ethylene glycol); gelatin; complex; gene delivery.

INTRODUCTION

The recent rapid development of molecular biology together with the steady progress of animal and plant genome projects has brought about some essential and revolutionary information on genes to elucidate all the biological phenomena at the molecular level [1–4]. In this situation, gene transfection is a key technology, indispensable to progress in molecular biology research [5–11]. Based on the

*To whom correspondence should be addressed. Tel.: (81-75) 751-4121. Fax: (81-75) 751-4646. E-mail: yasuhiko@frontier.kyoto-u.ac.jp

advent of genomics, new genes have been discovered and it is expected that they become therapeutically available for various diseases in near future. In this connection, gene therapy will be one of the new and promising medical therapies [12–16]. From the viewpoint of pharmaceutical sciences, it is necessary for successful gene therapy to achieve the delivery of genes to the target organ and tissue [17–20]. The objective of gene therapy is to allow a gene to express the coded protein in the target cells and consequently to treat disease by the protein secreted from transfected cells. Thus, it is important to develop a technology and methodology of a drug-delivery system to enhance the level of protein expression accompanied with gene transfection. For gene therapy, the viral gene carriers, such as adenovirus, retrovirus and adeno-associated virus, have been mainly used because of the high efficiency of gene transfection, although the clinical trials are quite limited by the adverse effects of virus itself, such as immunogenicity and toxicity or the possible mutagenesis of transfected cells. The new viral gene carrier with less adverse effects has been explored [21, 22], while the non-viral gene carrier has been investigated to enhance the transfection efficiency [6]. Comparable to the research and development of gene carriers, it will be important for *in vivo* gene therapy to control the body distribution of gene carriers and consequently that of gene complexed. When the complex of a plasmid DNA with a non-viral gene carrier is given to cells or injected into the body in the solution form, the plasmid DNA is rapidly and readily degraded and inactivated by enzymes or cells. As one practically possible way to minimize the enzymatic degradation of plasmid DNA, the surface of the plasmid DNA complex can be modified with polyethylene glycol (PEG) or PEG-like polymers. PEG has been chemically introduced to gelatin to prepare a PEG-introduced gelatin [23]. Following intravenous injection, the PEG-introduced gelatin was retained in the blood circulation for a longer time period than the original gelatin [23]. It is likely that gelatin is covered with PEG molecules and protected from the enzymatic attack and the exclusion by the reticuloendotherial system (RES).

Several synthetic materials, including cationic liposomes [24–26], poly(L-lysine) [27–30] and polyethylenimine [31–36], have been molecularly designed to demonstrate the successful DNA transfection into mammalian cells both *in vitro* and *in vivo*. Generally, since the plasmid DNA is a large and negatively charged molecule, it is impossible to allow the plasmid DNA to internalize into cells even though the attachment onto the cell membrane of negative charges takes place. When the plasmid DNA is polyionically complexed with synthetic cationic polymers, the molecular size of plasmid DNA decreases due to molecular condensation [37, 38]. It is likely that the condensed plasmid DNA–polymer complex of a positive charge can electrostatically interact with the cell membrane for internalization. Among the cationic polymers, it is known that the protonable amine residues of polyethylenimine could function as an endosomal buffering system which suppresses the action of endosomal enzymes to protect the plasmid DNA from degradation, the so-called buffering effect, resulting in the enhanced transfection efficiency [39].

Gelatin has been extensively used for industrial, pharmaceutical and medical applications. Its bio-safety has been proven through its long clinical usage as surgical biomaterial and drug ingredient. Another unique advantage is the electrical nature of gelatin which can be readily changed by the processing method of collagen for preparation [40]. For example, an alkaline processing allows collagen to structurally denature and hydrolyze the side chain of glutamine and asparagine residue. This results in generation of 'acidic' gelatin with an isoelectric point (IEP) of 5.0. On the other hand, an acidic processing of collagen produces 'basic' gelatin with an IEP of 9.0. We have prepared hydrogels by cross-linking gelatin for the controlled release of growth factors. Growth factors with IEP higher than 7.0, such as basic fibroblast growth factor [41], bone morphogenetic protein-2 [42], transforming growth factor beta1 [43] and hepatocyte growth factor [44], are immobilized into the biodegradable hydrogels of 'acidic' gelatin on the basis of the electrostatic interaction force between the growth factor and gelatin molecules. In this release system, the growth factor immobilized is not released from the gelatin hydrogel, unless the hydrogel carrier is degraded to generate water-soluble gelatin fragments. The growth factor release could be controlled only by changing the hydrogel degradation [41]. Depending on the nature of growth factors to be released, we can achieve their controlled release only if a biodegradable hydrogel is prepared from gelatin or the derivative which can physicochemically interact with the growth factor molecule. Another advantage of gelatin is to enable the chemical introduction with ease. For example, the cationized gelatin of positive charge can readily be prepared by introducing amine residues to the carboxyl groups of gelatin. The plasmid DNA polyionically immobilized in the cationized gelatin hydrogel is released from the hydrogel only if the hydrogel is degraded to generate the water-soluble degraded gelatin fragments [45, 46].

This study has been undertaken to evaluate the feasibility of a PEG-introduced cationized gelatin as a non-viral gene carrier. It is expected that PEG introduction (PEGylation) improves the biological stability of plasmid DNA against enzymatic attack, resulting in enhanced transfection efficiency *in vivo*.

MATERIALS AND METHODS

Materials

The gelatin sample with an IEP of 9.0 (MW = 10^5), prepared by an acid process of porcine skin, was kindly supplied by Nitta Gelatin (Osaka, Japan). 1-Ethyl-3-(3-dimethylaminopropyl) carbodiimide hydrochloride salt (EDC), β-alanine and 2,4,6-trinitrobenzensulfonic acid (TNBS) were purchased from Nacalai Tesque (Kyoto, Japan). Ethylenediamine was obtained from Wako (Osaka, Japan). Succinimidyl succinate-methoxy PEG (MW = 5000) was kindly provided by NOF (Tokyo, Japan).